

Elsevier Editorial System(tm) for Journal of Hydrology
Manuscript Draft

Manuscript Number: HYDROL13033R1

Title: Hydrologic and geochemical modeling of a karstic Mediterranean watershed

Article Type: Research Paper

Keywords: watershed modeling, karst, nitrates, climate change, Mediterranean

Corresponding Author: Dr. N.P. Nikolaidis,

Corresponding Author's Institution: Technical University of Crete

First Author: N.P. Nikolaidis

Order of Authors: N.P. Nikolaidis; Faycal Bouraoui, PhD; Giovanni Bidoglio, PhD

1 Hydrologic and geochemical modeling of a karstic

2 Mediterranean watershed

3

4 **N. P. Nikolaidis¹, F. Bouraoui² and G. Bidoglio²**

5 [1]{Department of Environmental Engineering, Technical University of Crete, Chania,

6 Greece; Tel: +30-28210-37785; Fax: +30-2821037846; e-mail:

7 nikolaos.nikolaidis@enveng.tuc.gr}

8 [2]{Institute for Environment and Sustainability, Joint Research Centre, European

9 Commission ISPRA(VA), Italy}

10 Correspondence to: N.P. Nikolaidis (nikolaos.nikolaidis@enveng.tuc.gr)

11

12 **Abstract**

13 The SWAT model was modified to simulate the hydrologic and chemical response of karstic

14 systems and assess the impacts of land use management and climate change of an intensively

15 managed Mediterranean watershed in Crete, Greece. A methodology was developed for the

16 determination of the extended karst area contributing to the spring flow as well as the degree

17 of dilution of nitrates due to permanent karst water volume. The modified SWAT model has

18 been able to capture the temporal variability of both karst flow and surface runoff using high

19 frequency monitoring data collected since 2004 and long term flow time series collected since

20 1973. The overall hydrologic budget of the karst was estimated and its evaporative losses were

21 calculated to be 28% suggesting a very high rate of karst infiltration. Nitrate chemistry of the

22 karst was simulated by calibrating a dilution factor allowing for the estimation of the total

1 karstic groundwater volume to approximately 500 million m³ of reserve water. The nitrate
2 simulation results suggested a significant impact of livestock grazing on the karstic
3 groundwater and on surface water quality. Finally, simulation results for a set of climate
4 change scenarios suggested a 17% decrease in precipitation, 8% decrease in ET and 22%
5 decrease in flow in 2030-2050 compared to 2010-2020. A tool for integrated water
6 management of karst areas has been developed, providing policy makers an instrument for
7 water management that could tackle the increasing water scarcity in the island.

8

9 **1 Introduction**

10 Continuous habitation in the past 12000 years of areas prone to water scarcity such as the
11 Mediterranean region has been primarily due to existence of reliable spring water supply
12 derived mostly from karstic formation natural reservoirs as well as the ability of land to
13 regenerate itself (Nikolaidis, 2011; Stamati et al., 2011). Karsts are derived from the
14 dissolution of limestone and dolomite formations and are comprised of a high transmissivity
15 fractured system of sinkholes, caves and springs. Such large, below-ground natural reservoirs
16 are very important in water resources management of the Mediterranean region because they
17 regulate water discharge of the karstic springs throughout the year (Moraetis et al., 2010;
18 Kourgialas et al., 2010). These water bodies will play a significant role in the overall rational
19 management of water resources of climate change impacted transitional areas such as the
20 Mediterranean where the precipitation is expected to decrease by at least 25% with increases
21 in the frequency of extreme events, and the average annual temperature to increase by 2-4° C
22 according to the IPCC (2007) scenarios. Warmer and drier conditions are expected to
23 intensify water shortages and cause loss in biodiversity and ecosystem services (Nikolaidis,
24 2011).

1 The importance of karstic aquifers in regional water management has been recognized by the
2 European Union (which prompted the creation of COST Action 620 to develop a
3 comprehensive risk based methodology for the sustainable management of karstic systems)
4 and the US EPA (which recognized the contribution of karst areas on the hydrology of
5 ephemeral and intermittent streams) and prompted the development of tools for sustainable
6 management (EC 2003; Levick et al., 2008). These water bodies will play a major role in
7 water management as they relate to water availability for potable water and agriculture (ie.
8 food security issues). Agriculture is a major driver in the management of water especially in
9 Mediterranean (Albiac et al., 2006; Wriedt et al., 2009) where 75% of the total agricultural
10 land is irrigated and it accounts for more than 60% of the total water abstractions (e.g. Spain
11 64%, Greece 88%, Portugal 80%).

12 A variety of karst models have been developed and applied to karst formation discharge
13 around the world. Recent attempts to model karstic discharge can be classified as follows: a)
14 conduit flow using Manning's equation, b) distributed groundwater model such as
15 MODFLOW, c) reservoir model, d) distributed hydrologic models coupled with conduit
16 routing and e) distributed parameters watershed models. Rozos and Koutsoyiannis (2006)
17 conceptualized conduit flow using Manning's equation and developed a multi-cell model
18 consisting of reservoirs and conduits in 3D. The model was applied to Almyros spring data
19 (eastern Crete, Greece) and the simulation results were compared with simulations of
20 MODFLOW. Similar comparison of a lumped karst model with MODFLOW was also
21 conducted by Martinez-Santos and Andreu (2010). Fleury et al., (2007) used a three reservoir
22 model to simulate successfully soil, slow discharge and rapid discharge of Fontaine de
23 Vaucluse karstic aquifer in southern France. A modified version of this model was used to
24 simulate Lez spring by incorporating active ground water management (Fleury et al., 2009). A
25 further improvement of such model was the incorporation of non-linear hysteretic discharge

1 functions that were applied to Vensim model by Tritz et al., (2011). Zhang et al., (2011)
2 modified a Distributed Hydrologic-Soil-Vegetation Model (DHSVM) to include flow routing
3 in karst conduits and model the hydrologic response of a small karst basin in southwest China.
4 Other distributed approaches to modeling karst hydrology were presented by Smaoui et al.,
5 (2011) that used the HySuf-FEM (Hydrodynamic of Subsurface Flow by Finite Element
6 Method) code to model the Berrechid karst aquifer in Morocco as well as Kurtulus and
7 Razack (2010) that used artificial neural network and adaptive neuro-fuzzy interface system
8 to model the daily discharge of the La Rochefoucauld karst aquifer in south-western France.

9 Distributed parameter watershed models such as SWAT (Soil and Water Assessment Tool,
10 Arnold et al., 1998) and HSPF (Hydrologic Simulation Program- FORTRAN, Bicknell et al.,
11 2001) have been used in the past to simulate the hydrologic response of karstic formations
12 (Spruill et al., 2000). Afinowicz et al. (2005) modified the aquifer discharge parameterization
13 of the SWAT model in order to better simulate the quick flow response of the karst in Texas
14 and Baffaut and Benson (2009) extended this parameterization by including sinkholes, losing
15 streams and return flow to model flow, fecal coliforms and phosphorus in a Missouri karstic
16 watershed. Tzoraki and Nikolaidis (2007) developed a two linear reservoir model to simulate
17 the karst and combined it with HSPF to simulate the hydrology, sediment transport and
18 nutrient loads of Krathis River basin in northern Peloponnese, Greece. Kourgialas et al.
19 (2010) added a distributed snow model to the karstic two reservoir model and combined it
20 with HSPF in order to simulate the hydrologic response of the Koiliaris River basin in Crete,
21 Greece.

22 The peculiarity of karst systems such as those found in the Mediterranean relies on the fact
23 that a spring could receive contributions from the karst that it is extended outside the
24 watershed boundaries to which the spring belongs as well as karsts situated one on top of the

1 other with different hydraulic characteristics and thus different transmissivities (EC 2004).
2 Identification of the extended karst area that contributes to the flow of the spring is extremely
3 important in order to obtain accurate hydrologic and geochemical balances of the system
4 (Tzoraki and Nikolaidis, 2007; Moraetis et al., 2010; Kourgialas et al., 2010). A second
5 peculiarity in artesian karstic systems has been discussed in detailed by Moraetis et al. (2010)
6 and deals with the diurnal variation of karst level. Barometric and temperature changes at the
7 entrance of the sinkhole create changes to the barometric pressure above the water table of the
8 karst, making it to operate as a bladder pump and introducing energy into the system which is
9 transformed into a highly dispersive system causing mixing and dilution of the pollutants.
10 Modeling of the geochemistry of the karst requires the determination of the degree of dilution
11 (i.e. volume of water within the karst below the level of spring discharge) in addition to spring
12 discharge.

13 The objective of this research was to study the hydrologic and chemical response of a karst
14 system in an intensively managed Mediterranean watershed in Crete, Greece and then assess
15 the impacts of land use management and climate change on the hydrologic and chemical
16 regime of the watershed. The SWAT model was modified to model the hydrologic and
17 chemical response of karst providing in this way policy makers a tool for integrated water
18 management that would tackle the increasing water scarcity in the island. We have selected to
19 model the nitrogen cycle as an indicator of both livestock and cultivation impacts on surface
20 and ground water quality (Glibert et al. (2006). Proper management of the nitrogen cycle in
21 intensively managed areas has become an urgent priority since it appears that nitrogen is one
22 of the planetary boundaries for safe operating space for humanity that has been exceeded
23 (Rockstrom et al., 2009).

24

1 **2 Watershed description and available data**

2 Koiliaris River watershed is located in the north-western part of Crete near Chania, Greece
3 and has a watershed area of 132 km² (Fig. 1). Based on the geomorphologic characteristics of
4 the basin, hydrologic modeling and the orientation of the fault system, the extended karst area
5 that contributes to the spring flow in the watershed was located south east of the area and was
6 estimated to include at least 50 Km² (Moraetis et al., 2010). The watershed has an intense
7 geomorphology with elevations ranging from 0 to 2120 m AMSL and slopes ranging from
8 43% (at high elevations) to 1-2% (valley). The predominant geologic formations are:
9 limestones, dolomites, marbles, and re-crystallized limestones with cherts of the Plattenkalk,
10 Tripolis, and Trypali series (71.8%), calcareous marls and marls - Neogene deposits (15.6%),
11 schists (6.1%) and quaternary alluvial deposits (6.4%).

12 The karstic system of the White Mountains is comprised of an autochthonous geotectonic
13 unit, Plattenkalk (Metamorphic Crystalline Limestones - Mesozoic period) and two
14 allochthonous units, the Trypali limestones (Triassic to Cretaceous period) and the
15 metamorphic schists (Fig. 1). The Plattenkalk nappe consists of layers of dolomites,
16 limestones and marbles and limestone and cherts with intense bedding (in the lower boundary
17 of metamorphism). The Trypali nappe is highly karstified and has overthrust the
18 Plattenkalk nappe. The metamorphic schists overthrust both the Plattenkalk and Trypali
19 units mainly in the western part of the White Mountains. Neogene sediments (marls and
20 marly limestones) have been deposited at the lower elevations of the basin over the
21 autochthonous formation. Finally, alluvial sediments are found near the river corridor mostly
22 in lower elevations. Fig. 1 presents the geology of the area of Koiliaris River watershed and
23 Fig. 2 presents two geologic cross sections depicting the stacking of the nappes and the
24 existing faults.

1 The stratigraphy of Crete has been formed by one dipping north and one south that meet at the
2 north-south divide (approximately at 2000 m elevation) as well as east-west trending zones
3 (Papanikolaou and Vassilakis, 2010). The Plattenkalk autochthonous formation in the
4 watershed has significant east-west normal faults dipping north. At the eastern part of the
5 White Mountains there is increased exhumation of the autochthonous nappes, while in the
6 western part, there is stacking of allochthonous nappes that overthrust the north-west dipping
7 of Plattenkalk. Along the Plattenkalk dipping a series of normal faults influence the creation
8 of neogene sedimentary basins (Fassoulas, 1999).

9 The karst system is characterized by very fast infiltration and direct connection to the conduits
10 below. There is a significant number of sinkholes with long downward shafts, caves and a
11 deep conduit system (Gourgouthakas cave -1205m, Lontari cave -1100m; Moraetis et al.
12 2010). The karst system discharges in a series of permanent springs, Stylos springs at
13 elevation +17 m AMSL and an intermittent spring, Anavreti at elevation +24 m AMSL. Both
14 springs then feed Koiliaris River. The springs have an average discharge of 154 million m³/yr
15 (2007-2010) with very intense fluctuation between winter and summer flows. The total
16 recharge area of the springs extend beyond the boundaries of Koiliaris River Basin to the
17 south-east of the watershed boundary (Moraetis et al., 2010). The area of the extended karst
18 is depicted in Fig. 1 and was determined based on geologic and fault analysis (Fig. 2). The
19 cross sections of the extended karst area identify a major fault in a northeast-southwest
20 direction (located at the boundary of the karst and neogene deposits) which together with
21 dipping of the nappes direct the water towards the Koiliaris River Basin. Considering the
22 dipping of Plattenkalk nappes towards north-west in relation to normal faulting, the dolomites
23 (lower part of the stacking sequence) which are less karstified come in contact with the
24 Plattenkalk nappes (upper part - more karstified limestones with cherts) at lower elevation
25 (Fig. 2) directing the water to the springs.

1 The approximate location of the extended karst of Stylos springs (the main spring in Koiliaris
2 River Basin) was presented in Moraetis et al. (2010) and there have been a series of published
3 (Papanikolaou and Vassilakis, 2010) and unpublished studies (i.e. tracer studies conducted by
4 Institute of Geological and Metallurgical Research, Knithakis, 1993 and bore log sections
5 from speleological exhibitions in the main/large caves and sinkholes) that describe the setting
6 of the karst in the area. One of the problems of using tracer studies in a geologic setting such
7 as Stylos Karst in order to delineate the extended karst area is the high degree of dilution due
8 to the large volume of discharge water (80-150 Mm³/yr) and the permanent volume.

9 There are two episodic and one temporary tributaries in the basin and they are joined by
10 Stylos spring discharge to make the permanent reach of Koiliaris River. The two episodic
11 tributaries drain the karst area (north-east part of the watershed), while the episodic tributary
12 flows initially over schist formations before it enters a karstic gorge situated along a fault
13 (Diktamos Gorge). The confluence of the three tributaries is located in the alluvial deposits of
14 the valley.

15 The agricultural land consists of olive groves, citrus groves, vines and vegetables (32.1 %)
16 grown with conventional practices such as tilling, irrigation and use of fertilizers. Intensively
17 grazed scrubland/pasture by livestock covers large areas (67.3 %) of the watershed at high
18 altitudes and forest (0.6%). The composition of land use has not changed in the past 50 years,
19 however, the intensity of use has changed significantly. For instance, the number of animals
20 grazing in the watershed and its extended karst increased from about 23393 sheeps and goats
21 in 1961 to 123987 in 2001. Since the grazing area remained relatively constant (16875 ha),
22 the grazing intensity changed from a level of 1.4 animals/ha to 6.8 animals/ha. Similarly, the
23 cultivation of agricultural land has been intensified with increasing fertilizer application.
24 Using country statistics, fertilizer consumption rose steadily from 159000 tn/yr in 1960 to

1 710000 tn/yr in 1990 and then it has been dropping to 405000 tn/yr in 2002. Intensive
2 cultivation and livestock grazing have deteriorated significantly soil quality and land fertility.
3 Soils are thin, poorly developed, following the lithology of the area. There are three main
4 types of soils: in high altitude, there are calcaric Lithosols (FAO) obtained from the
5 weathering of limestones, the calcaric regosols developed in low altitudes in Neocene and
6 Alluvial formations and the eutric lithosols developed in schists with mainly coarse texture.

7 The Region of Crete in collaboration with the Prefecture of Chania have been conducting
8 meteorological and hydrologic monitoring of precipitation (daily), air temperature (daily),
9 spring flow (on a monthly basis) since 1973. The Technical University of Crete augmented
10 this network and in 2004 initiated hydrologic and geochemical monitoring of the Basin
11 consisting of a continuous telemetric monitoring gauging station (five minutes to 1 hour
12 interval) in Koiliaris river (R1), level loggers at the entrance and exit of the gorge (R2 and
13 R3), water level and temperature logger at the Macheri well (G1) and two meteorological
14 stations (M1 and M2) at elevations of 950 m and 300 m AMSL (Fig. 1). The sensors included
15 in the telemetric gauging station (R1) include pH, nitrate (NO_3^- -N), water temperature ($^{\circ}\text{C}$),
16 dissolved oxygen (mgL^{-1}) and river stage (m) (multi-parameter Troll9500 by In Situ Inc.). In
17 addition to the telemetric data, monthly field campaigns are conducted for both surface and
18 ground water quality measurements. Further details on the monitoring network and data
19 analysis can be found in Moraetis et al. (2010).

20

21 **3 SWAT model description and modifications**

22 SWAT is a deterministic, continuous time (daily time step) basin scale model that was
23 designed to simulate the hydrology, sediment yield and water quality (nutrient and pesticides)
24 of ungauged watersheds (Arnold et al., 1998) and evaluate the impact of agricultural

1 management practices on water quality and agricultural yields. The watershed is first
2 subdivided into subcatchments and each subcatchment into hydrologic response units (HRU)
3 that are a function of soil type, land use and land slope. The model has incorporated the
4 following components: weather generator routine, hydrologic mass balance, soil temperature
5 and soil properties, plant growth, nutrients, pesticides, bacteria and pathogen mass balances,
6 and land management practices. The hydrologic component of each HRU includes the
7 following processes: evapotranspiration, plant uptake, surface runoff and infiltration (using
8 the modified Curve Number or the Green-Ampt method), percolation, lateral subsurface flow,
9 groundwater return flow from the shallow aquifer, deep aquifer losses and channel
10 transmission loss subroutines. Water balance is conducted for the snow compartment, soil,
11 shallow aquifer and deep aquifer. Plant growth is based on the EPIC crop model and uses the
12 "heat units" concept which relates crop growth to the excess of daily temperature above a base
13 temperature. Potential evapotranspiration, leaf area index, rooting depth and soil water
14 content determine the water uptake of plants.

15 In order to be able to simulate the contribution of the extended karst to the discharge of a spring
16 as well as account for the variability of the recession of the discharge due to two karst
17 formations, we augmented SWAT by using (in series) a modified version of the karst flow
18 model described by Tzoraki and Nikolaidis (2007) and Kourgialas et al. (2010). A brief
19 description of the modified karst model follows (Fig. 3). The major modifications from the
20 previous versions are: a) the input flow is the deep groundwater flow from SWAT and b) a
21 nitrate-N mass balance was included assuming that nitrate is conservative in the karst. The
22 hydrologic mass balances of the karst model are:

23 Upper Reservoir Mass Balance

24
$$\frac{dV_1}{dt} = Q_{in,1} - Q_1 \quad (1)$$

1 Lower Reservoir Mass Balance

2
$$\frac{dV_2}{dt} = Q_{in,2} - Q_2 \quad (2)$$

3 Where:

4
$$Q_{in,1} = a_1 * Q_{in,deepGW}$$

5
$$Q_{in,2} = (1-a_1) * Q_{in,deepGW} + a_2 * Q_1$$

6
$$Q_1 = K_u * V_1$$

7
$$Q_2 = K_l * V_2$$

8 and $Q_{in,deepGW}$ is the deep groundwater flow from SWAT, a_1 is the fraction of karst with the
9 upper reservoir, a_2 is the fraction of flow from the upper reservoir discharge entering the
10 lower reservoir and K_u and K_l are recession constants (1/d) for the upper and lower reservoir.

11 For constant $Q_{in,1}$ and $Q_{in,2}$ (daily time step) the analytical solutions of 1 and 2 follow:

12
$$Q_1 = Q_{1,0}e^{-kut} + Q_{in,1}(1 - e^{-akut}) \quad (3)$$

13
$$Q_2 = Q_{2,0}e^{-kl(1-a_2)t} + (1-a_1)Q_{in,2}(1 - e^{-kl(1-a_2)t}) \quad (4)$$

14 The total karstic flow is calculated as:

15
$$Q_{karstic} = (1-a_2)Q_1 + Q_2 \quad (5)$$

16 In a similar fashion, the nitrate-N mass balances are:

17 Upper Reservoir Mass Balance

18
$$\frac{d(V_1 * C_1)}{dt} = a_1 * Q_{in,1} * C_{in,1} - Q_1 * C_1 \quad (6)$$

19 Lower Reservoir Mass Balance

20
$$\frac{d(V_2 * C_2)}{dt} = (1-a_1) * Q_{in} * C_{in} + a_2 * Q_1 * C_1 - Q_2 * C_2 \quad (7)$$

21 The mass balance equations were solved analytically for a daily input time step. Given that
22 the volume of the two reservoirs reflect the daily volume corresponding to the discharging

1 water from the spring and does not account for the permanent volume of the karst below the
2 spring level, a deep karst factor was introduced in the model equation of the lower reservoir to
3 account for the extra dilution of the incoming chemical loads and in this way provide an
4 estimate of the total volume of the karst. Moraetis et al. (2010) discussed in detail the
5 fluctuation of the karst water level which introduces significant dispersion in the system and
6 thus mixing of the incoming loads.

7 An spreadsheet version of the karstic model was used for this study in order to facilitate
8 model calibration as well as sensitivity and uncertainty analysis. The precipitation in the
9 karstic area of the watershed was directed to deep groundwater after allowing SWAT to
10 simulate surface hydrologic processes such as snow accumulation and melt, surface runoff,
11 infiltration to shallow groundwater and evapotranspiration. The deep groundwater flow of the
12 karstic area that could be attributed to a specific spring (based on fault analysis and other
13 available data and observations) was aggregated on a daily basis and was input to the two-part
14 reservoir karst model. The karst model parameters were calibrated and the resulting time
15 series were used as point source input at the spring. A methodology was developed to
16 quantify the extent of the karst (as determined by geologic analysis) by using mass balance
17 modeling. The quantification was determined by "trial and error", which in practice was
18 assigning areas from the extended karst to contribute to Stylos spring discharge, i.e. including
19 or excluding different HRUs deep groundwater flows. Once the karst model parameters were
20 calibrated, the spreadsheet could be connected to a risk analysis software (@RISK by
21 PALISADE) to conduct easily sensitivity and uncertainty analysis due to model parameters.

22 Three years of hydrologic and water quality data from 2007 until 2010 were used in order to
23 calibrate the model. The data included a complete data set of flow measurements at the
24 watershed outlet, flow data of Keramianos tributary at the gorge entrance and exit for 2007-

1 2008, grab sample data for nitrates at Keramianos tributary, the watershed outlet and
2 groundwater wells and continuous high frequency nitrate data (converted to flow weighted
3 daily average values) at the watershed outlet. The verification (Refsgaard, 1997) of the
4 hydrologic calibration was obtained using watershed data from 2004 to 2007 as well as spring
5 flow monthly measurements from 1973 to 2004 for two out of the three springs of the
6 watershed. The two springs measured are located at the community of Stylos and the third
7 spring (Anavreti) at the community of Nio Chorio. Anavreti is an intermittent spring that runs
8 for a few months between December and March. Existing nitrate grab sample measurements
9 between 2004 and 2007 were used for the verification of the nitrate simulation.

10 The methodology used for model calibration followed a three step approach. First the
11 hydrologic parameters of the subbasins contributing to Keramianos tributary surface runoff
12 were calibrated. Then the transmission losses through the gorge were adjusted and finally, the
13 Stylos spring flow was calibrated using the methodology outlined earlier for the determination
14 of the extended karst.

15 The combination of General Circulation Models (GCM) [ECHAM5 (Roeckner, 2003); BCA
16 (Déqué et al., 1994)] and three Regional Circulation Models (RCM) [RACMO2 (van
17 Meijgaard et al., 2008); RCA (Kjellstrom et al., 2005); REMO (Jacob, 2001) were selected
18 for climate change scenarios. They are based on the A1B storyline. The A1 family of
19 scenarios is based on rapid economic growth, an increase in population until the mid-century
20 and a decrease thereafter and the introduction of new and more efficient technologies. The
21 scenario A1B puts a balanced emphasis on all energy sources (IPCC, 2000). The three
22 combinations used were ECHAM-RACMO, BCA-RCA and ECHAM_REMO. All time series
23 covered the time period 1990-2050. All climate change time series were biased corrected as
24 detailed by Rojas et al. (2011).

1

2 **4 Results and discussion**

3 The region surrounding Koiliaris River basin was delineated into 41 subbasins using as
4 criterion the elemental catchment of 500 ha and 160 hydrologic response units (HRUs).
5 Koiliaris River basin had a surface area of 132 km² and it was divided into 8 subbasins and 27
6 HRUs while the contributing extended karst had a surface area of 79 Km² (11 subbasins and
7 28 HRUs) . Time series from 6 precipitation stations were used to synthesize 37 years of
8 precipitation record (1973-2010) by filling missing data using cross station regressions. The
9 density of the precipitation network and the location of the stations (3 within the watershed at
10 3 different elevations and 3 stations outside the watershed) were able to account for the
11 orographic variability of rainfall. On the other hand, a 37 year long record was synthesized
12 for two temperature stations and a temperature gradient of -5.6° C/1000m elevation was used
13 to adjust the daily temperature record in every subbasin and account for the orographic effect.
14 The elevation band feature of the SWAT model was activated in order to better capture the
15 snow/rain distribution in the basin.

16 **Hydrologic simulation:** The annual areal weighted precipitation for the calibration period
17 over the watershed and the extended contributing karst was 1363 mm/yr while the actual
18 evapotranspiration was estimated to be 455 mm/yr. Snow covered an area of 82 km² and
19 melted within a few days at low elevations and 100-140 days at high elevations respectively.
20 Snow cover typically started in early December and lasted until early May. The annual
21 average outflow of Koiliaris River Basin was estimated to be 621 mm/yr (131 Mm³/yr). A
22 comparison between simulated flows and observed flows at three stations in the watershed is
23 presented in Fig. 4. The annual average flow at the gorge entrance was estimated to be 12.5
24 Mm³/yr. Using 240 days daily flow data, the root mean squared error (RMSE) was estimated

1 to be 0.087 m³/s and the closure of the cumulative simulated flow and observed flow was
2 15%. The annual average flow at the gorge exit was estimated to be 2.2 Mm³/yr due to
3 transmission losses. The RMSE was estimated to be 0.048 m³/s. Finally, the annual average
4 flow at the basin's outlet (Koiliaris gauging station) was estimated to be 131 Mm³/yr, 118
5 Mm³/yr from Karst and 13 Mm³/yr from surface runoff. The RMSE was estimated to be 2.9
6 m³/s and the closure of the cumulative simulated flow and observed flow was 2.6%. The
7 mean daily observed flow was 4.25 m³/s (5.32 m³/s standard deviation) while the mean daily
8 simulated flow was 4.14 m³/s (5.24 m³/s standard deviation). The coefficient of
9 determination between observed and simulated flows was 0.72 and the slope 0.89. The
10 goodness of fit of the calibration period was examined using the statistics suggested by
11 Moriasi et al. (2007), namely the Nash-Sutcliffe Efficiency (NSE), Percent Bias (PBias), and
12 RMSE Standard Deviation Error (RSR). A simulation is considered adequate if NSE>0.5,
13 Pbias < ±25% and RSR<0.7. These statistics were calculated using the daily record and the
14 monthly average record. The NSE was 0.62, PBias -22.3 and RSR 0.62 for the daily record
15 and 0.77, -22.1 and 0.48 for the monthly record. The goodness of fit of the calibration was
16 considered adequate since all three statistics were passed for both daily and monthly record.

17 The overall hydrologic budget of Keramianos sub-basin that is characteristic mostly of a
18 schist geologic bedrock was the following. The annual average precipitation and snow melt
19 was 1209 mm/yr, ET was 567 mm/yr and the runoff was 547 mm/yr. The runoff coefficient
20 of the basin was 45%. The overall hydrologic budget of the karst was the following. The
21 annual average precipitation and snow melt was 1494 mm/yr, ET was 418 mm/yr and the
22 spring runoff was 803 mm/yr. The runoff coefficient of the karst was estimated to be 54%.
23 The evaporative losses of the karst were estimated to be 28% suggesting a very high rate of
24 karst infiltration which could be justified by the very thin soils, sparse vegetation at high
25 elevation and intense karstification of the Tripali zone.

1 Model verification was achieved using an independent record of flows (2004-2007) and
2 simulating the whole basin. A comparison between simulated flows and observed flows at
3 the Koiliaris gaging station is presented in Fig. 5. The goodness of fit statistics of the
4 verification period were the following. The NSE was 0.43, PBias -11.6 and RSR 0.75 for the
5 daily record and 0.61, -11.8 and 0.63 for the monthly record. The goodness of fit of the
6 verification simulation was considered adequate for the monthly record since all three
7 statistics were passed, but not for the daily record. In addition, a qualitative verification of the
8 hydrologic simulation was conducted using monthly flow measurements since 1973 of two of
9 the three outlet points of the Stylos spring. The simulated flows compare very well with the
10 observed data for 8-9 out of the 12 months confirming the goodness of fit of the hydrologic
11 simulation using this long term record (Fig. 5b).

12 A sensitivity and uncertainty analysis was conducted by combining the karstic model with
13 @RISK, a risk analysis software in order to determine the uncertainty of the four model
14 parameters controlling discharge. We assumed that the parameter had a uniform distribution
15 $\pm 50\%$ of their respective calibrated value. We run 1000 Monte Carlo simulations and
16 calculated the distributions on the monthly average discharge for 2008-2009 hydrologic year.
17 The most sensitive parameters in ranking order were: K_l , the recession constants for the lower
18 reservoir, a_2 , the fraction of flow from the upper reservoir discharge entering the lower
19 reservoir, a_1 , the fraction of karst with the upper reservoir, and K_u , the recession constants for
20 the upper reservoir. The uncertainty (95% confidence level) of the simulation results due to
21 model parameters ranged from 0.2-5.8% of the monthly average discharge.

22 **Nitrate simulation:** Nitrogen inputs in the watershed and its extended karst were calculated
23 as follows. Nitrate-N atmospheric deposition was estimated to 11.5 Kg/ha/yr using a
24 measured average rainfall concentration for nitrate-N of 0.91 mg/L and a dry deposition of

1 inorganic nitrogen of 6 Kg/ha/yr. Inorganic fertilization and livestock manure contributed
2 18.3, 10.1 and 17.4 Kg/ha/yr of nitrate-N, ammonia-N and organic-N respectively. Inorganic
3 fertilization was applied (using a 30-15-0 fertilizer) at a rate of 80 Kg/ha for olive groves, 70
4 Kg/ha for citrus and vines and 220 Kg/ha for other crops. Manure was applied to pasture and
5 forested areas depending on the livestock density using OECD excretion rates of 10 Kg-
6 N/head/yr and 260 Kg manure/head/yr for sheeps and goats. The application rates were
7 estimated then to be 110 Kg/ha/mo in the municipality of Armenoi, 150 kg/ha/mo in the
8 municipalities of Fre and Krionerida and 200 Kg/ha/mo in the municipality of Keramia.
9 Nitrate uptake was estimated to be 41.94 Kg/ha from the simulation. Nitrate-N export to the
10 sea was estimated to be 284 tn/yr or 13.5 Kg/ha/yr. A comparison of the simulated nitrate
11 concentration at the gorge entrance and at the basin's outlet (Koiliaris gaging station) is
12 presented in Fig. 6. In order to simulate the chemistry of the karst, for the reasons explained
13 earlier in the model development, a deep karst factor was assumed of 4.5. This means that the
14 total volume of the karstic reservoir is 4.5 times the annual flow of the springs. This brings
15 the estimate of the total groundwater volume within the watershed and the extended karst
16 contributing to the spring to approximately 500 million m³ of reserve water. There are very
17 few grab sample data to compare with the simulation results at the entrance of the gorge,
18 however, the simulation has captured the variability of the data. A better statistical analysis of
19 the results was conducted at the main gaging station. The mean daily observed nitrate
20 concentration was 1.2 mg/L (0.56 mg/L standard deviation) while the mean daily simulated
21 nitrate concentration was 1.11 mg/L (0.41 mg/L standard deviation). The RMSE of the
22 simulation was 0.57 mg/L. The nitrate simulation passed through +/- one standard deviation
23 of the observed data 80% of the time on a monthly basis. The results suggest a significant
24 impact of livestock grazing on the karstic groundwater and on surface water quality.
25 Livestock manure accumulates on the soil/karst surface during the dry period and it is flushed

1 out during the first rainfall events in the fall, raising the nitrate-N concentrations in
2 groundwater to 8 mg/L.

3 A separate sensitivity and uncertainty analysis was conducted in order to determine the
4 uncertainty of the four hydrologic parameters and one chemical parameter (deep karst factor)
5 controlling nitrate concentrations. It was assumed that each parameter had a uniform
6 distribution $\pm 50\%$ of their respective calibrated value and 1000 Monte Carlo simulations
7 were used to calculate the distributions of the monthly average nitrate concentration for the
8 hydrologic year 2008-2009. The uncertainty (95% confidence level) of the simulation results
9 of nitrate concentrations due to the four hydrologic parameters and one chemical parameter
10 was very low and on average 0.12% of the monthly average nitrate concentration. The tight
11 confidence level of the nitrate simulation results suggests that the calibrated parameters
12 (including the deep karst factor) were very close to their optimal value as well as the
13 uniqueness of the solution.

14 The results from the various aspects of the modeling exercise have been consistent,
15 corroborating with the hypothesis of the deep karst factor as a dilution factor of water quality
16 as well as with the quantification of the extended karst and thus the "karst water reserves"
17 using the mass balance equations of a hydrologic model. The theoretical estimation of "karst
18 water reserves" can be further tested by modeling other natural substances such as the
19 chloride ion or isotopes that act as conservative tracers.

20 **Hydrologic hindcasting simulations:** A trend analysis of precipitation, temperature and flow
21 for the existing 37 year record showed the following. There has been a decreasing trend in
22 precipitation on an annual basis as well as 3 out of the six wet months (October, January and
23 March). The maximum temperature has no trend on an annual basis and increasing trend for
24 the months of August through October and decreasing for January and February. The

1 minimum temperature has an increasing trend on an annual basis as well as for all the months
2 of the year.

3 The SWAT model has simulated 74 flood events at the gorge exit. Fig. 7a presents the daily
4 simulated hydrograph at that location. The frequency distribution of flood events has not
5 changed with time however, the intensity of the flood has changed significantly through the
6 years. Prior to the drought years of 1988 and 1991 (1973-1992), there were 37 flood events
7 with average maximum flood flow at the exit of the gorge of 1.7 m³/s, while from 1993-2010,
8 there were 38 flood events with average maximum flood flow of 4.3 m³/s (2.5 times higher).
9 Fig. 7b presents the frequency distribution of maximum flood flows at the same location using
10 all flood events and Fig. 7c presents the distributions for two distinct periods, 1973-1996 and
11 1997-2010. There has been a significant shift in the frequency of the maximum floods
12 towards higher intensity, which is in agreement with the trend analysis of precipitation and
13 temperature.

14 **Future scenarios:** Fig. 8 presents the predictions of annual precipitation, actual ET and
15 runoff for Koiliaris River Basin under the a) BCM_RCA, b) ECHAM_RACMO, and c)
16 ECHAM_REMO climate change scenarios for the 1990-2050. All three scenarios give
17 consistent results, predicting significant decreases in annual precipitation, actual ET and
18 runoff after 2030. In order to quantify the changes due to climate, given the local decadal
19 climatic variability, we calculated 20-year average (and standard deviation) from the three
20 climate change scenarios for precipitation, actual ET and flow for Koiliaris River Basin (based
21 on model simulations, see Fig. 9). The results suggest a 17% decrease in precipitation, 8%
22 decrease in ET and 22% decrease in flow in 2030-2050 compared to 2010-2029. These
23 differences are statistically significant ($p=0.05$, two sided, unequal variance) based on t-
24 testing. In addition, model simulations show nitrate concentrations proportionally increasing
25 due to decreasing flow and constant nitrate load in the basin. Climate change will exacerbate

1 the problems of water scarcity and water quality in the region that will be pronounced in the
2 summer months and during the first flush in the fall respectively.

3

4 **5 Conclusions**

5 The modified SWAT model has been able to capture the temporal variability of both karstic
6 flow and surface runoff using high frequency monitoring data collected since 2004, the long
7 term flow time series collected since 1973 as well as the variability of nitrate concentrations as
8 a proxy to land use impacts. A methodology was developed to quantify the extent of the karst
9 (as determined by geologic analysis) by using mass balance modeling which in combination
10 with nitrate modeling in the karst provided additional consistent evidence. The results of this
11 study can be summarized as follows:

- 12 • The overall hydrologic budget of the karst was estimated and its evaporative losses
13 were 28% suggesting a very high rate of karst infiltration.
- 14 • Nitrate chemistry of the karst was simulated by calibrating a deep karst factor (4.5)
15 which allowed for the estimation of the total karstic groundwater volume to
16 approximately 500 million m³ of reserve water. The nitrate simulation results
17 suggested a significant impact of livestock grazing on the karstic groundwater and on
18 surface water quality. Livestock manure accumulated on the soil/karst surface during
19 the dry period and it is flushed out during the first rainfall events in the fall, raising the
20 nitrate-N concentrations in groundwater to 8 mg/L. In addition, nitrate-N export to the
21 sea was estimated to be 284 tn/yr or 13.5 Kg/ha/yr impacting the coastal zone.
- 22 • The SWAT model simulated 74 flush flood events that occurred in 37 years. There
23 has been a significant shift in the frequency of the maximum floods towards higher
24 intensity (1973-1996 vs. 1997-2010), which is in agreement with the trend analysis of
25 precipitation and temperature.

- 1 • Finally, climate change simulation results suggested a 17% decrease in precipitation,
2 8% decrease in ET and 22% decrease in flow in 2030-2050 compared to 2010-2029.
3 Climate change will exacerbate the problem of water scarcity in the region that will be
4 pronounced in the summer months.

5 This study has shown that Koiliaris River Basin is already experiencing the impacts of climate
6 change in the past 50 years while land use practices (especially of livestock grazing) have
7 impacted adversely surface and ground water quality. A tool for integrated water management
8 has been developed, providing policy makers with an instrument for water management that
9 could tackle the expected decrease of water availability in the Koiliaris River basin and the
10 increasing water scarcity in the island.

12 **Acknowledgements**

13 Funding for this work was provided by the EU FP7-ENV-2009 Project SoilTrEC “Soil
14 Transformations in European Catchments” (Grant #244118). This work was conducted at the
15 Institute for Environment and Sustainability of the Joint Research Centre (JRC) of the
16 European Commission. Professor Nikolaidis is grateful for the Technical University of Crete
17 financial support of his sabbatical leave at the JRC.

19 **References**

20 Afinowicz, J. D., Munster, C. L., Wilcox, B. P.: Modeling effects of brush management on
21 the rangeland water budget: Edwards Plateau, Texas, JAWRA, 41, 181-193, 2005.
22 Albiac, J., Martinez, Y., Tapia, J.: Water quantity and quality issues in the Mediterranean
23 agriculture, In: OECD Workshop on Agriculture and Water Sustainability, Markets and
24 Policies, Session 2, 2006.

1 Arnold, J. G., Srinivasan, R., Muttiah, R. S. and Williams, Jr.: Large-area hydrologic
2 modeling and assessment: Part I. Model development, Journal of American Water Resources
3 Association, 34, 73–89, 1998.

4 Baffaut, C. and Benson, V. W.: Modeling flow and pollutant transport in a karst watershed
5 with SWAT, Transactions of the ASABE, 52, 469-479, 2009.

6 Bicknell, B.R., Imhoff, J.S., Kittle, J.L., Jobes, T.H. and Donigian, A.S.: Hydrological
7 Simulation Program – FORTRAN (HSPF): User’s Manual – Version 12, National Exposure
8 Research Laboratory, Office Of Research And Development, U.S. Environmental Protection
9 Agency, Athens, Georgia, USA, 2001.

10 Debele, B., Srinivasan, R., Parlange, J-Yves: Hourly Analyses of hydrological and water
11 quality simulations using the ESWAT Model, Water Resources Management, 23, 303-324,
12 2008.

13 Déqué, M., Drevet, C., Braun, A., Cariolle,,: The ARPEGE/IFS atmosphere model: a
14 contribution to the French community climate modeling. Climate Dynamics, 10 (4-5), 249-
15 266, 1994.

16 EC: The main coastal karstic aquifers of southern Europe. Ed: Calaforra, J. M., COST-621
17 Action "Groundwater management of coastal karstic aquifers", European Commission, DG-
18 Research, pp 126, 2004.

19 EC: Vulnerability and risk mapping for the protection of carbonate (Karst) aquifers. Ed:
20 Zwahlen, F., COST-620 Action Final Report, European Commission, DG-Research, pp 320,
21 2003.

22 Fassoulas, C., The structural evolution of central Crete: Insight into the tectonic evolution of
23 the South Aegean (Greece). Journal Geodynamics, 27, 23-43, 1999

1 Fleury, P., Ladouche, B., Conroux, Y., Jourde, H., and Dorfliger, N.: Modelling the
2 hydrologic functions of a karst aquifer under active water management - The Lez spring,
3 Journal of Hydrology, 365, 235-243, 2009.

4 Fleury, P., Plagnes, V., and Bakalowicz, M.: Modelling the functioning of karst aquifers with
5 a reservoir model: Application to Fontaine de Vaucluse (South of France), 345, 38-49, 2007.

6 Glibert, P. M., Harrison, J., Heil, C. and Seitzinger, S.: Escalating worldwide use of urea - a
7 global change contributing to coastal eutrophication, Biogeochemistry, 77, 441-463, 2006.

8 Emissions scenarios. A special report of Working Group III of the International Panel on
9 Climate Change. Cambridge University Press, 2000.

10 Jacob, D.:The role of water vapor in the atmosphere. A short overview from a climate
11 modeller's point of view. Phys. Chem. Earth, 26A, 523-527.

12 Kjellström, E., Bärring, L., Gollvik, S. and Hansson, U.: A 140-year simulation of European
13 climate with the new version of the Rossby Centre regional atmospheric climate model
14 (RCA3). Rep. Meteorol Climatol, 108, SMHI, Norrköping, Sweden, 2005.

15 Kourgialas, N. N., Karatzas, G. P. and Nikolaidis, N. P.: An integrated framework for the
16 hydrologic simulation of a complex geomorphological river basin, Journal of Hydrology, 381,
17 308-321, 2010.

18 Kourtulus, B., and Razack, M.: Modeling daily discharge responses of a large karstic aquifer
19 using soft computing methods: Artificial neural network and neuro-fuzzy, Journal of
20 Hydrology, 381, 101-111, 2010.

21 Levick, L., Fonseca, J., Goodrich, D., Hernandez, M., Semmens, S., Stromberg, J., Leidy, R.,
22 Scianni, M., Guertin, D. P., Tluczek, M. and Kepner, W.: The ecological and hydrological
23 significance of ephemeral and intermittent streams in the arid and semi-arid American
24 Southwest, U.S. Environmental Protection Agency and USDA/ARS Southwest Watershed
25 Research Center, EPA/600/R-08/134, ARS/233046, 116 pp, 2008.

1 Martinez-Santos, P., and Andreu, J.M.: Lumped and distributed approaches to model natural
2 recharge in semiarid karst aquifers, *Journal of Hydrology*, 388, 389-398, 2010.

3 Moraetis, D., Stamati, F., Kotronakis, E., Fragia, T., Paranychnianakis, N. and Nikolaidis, N.
4 P.: Identification of hydrologic and geochemical pathways using high frequency sampling,
5 REE aqueous sampling and soil characterization at Koiliaris Critical Zone Observatory,
6 *Applied Geochemistry*, 26, S101-S104, 2011.

7 Moraetis, D., Efstathiou, D., Stamati, F., Tzoraki, O., Nikolaidis, N. P. Schnoor, J. L. and
8 Vozinakis, K.: High frequency monitoring for the identification of hydrological and
9 biochemical processes in a Mediterranean river basin, *Journal of Hydrology*, 389, 127-136,
10 2010.

11 Nikolaidis, N.P.: Human impacts on soil: Tipping points and knowledge gaps, *Applied*
12 *Geochemistry*, 26, S230-S233, 2011.

13 Nikolaidis, N. P., Karageorgis, A., Kapimalis, V., Drakopoulou, P., Skoulikidis, N., Behrendt,
14 H. and Levkov, Z.: Management of nutrient emissions of Axios river catchment: their effect
15 in the coastal zone of Thermaikos gulf-Greece, *Ecological Modeling*, 220, 383–396, 2009.

16 Papanikolaou, D., Vassilakis, E., Thrust Faults and Extensional Detachment Faults in Cretan
17 Tectono-stratigraphy: Implications for Middle Miocene Extension. *Tectonophysics*, 488, 233-
18 247. 2010

19 Smaoui, H., Zouhri, L., Ouahsine, A., and Carlier, E.: Modelling of groundwater flow in
20 heterogeneous porous media by finite element method, *Hydrological Processes*, DOI:
21 10.1002/hyp.8156 (published on-line).

22 Spruill, C.A., Workman, S. R. and Taraba J.L.: Simulation of daily and monthly stream
23 discharge from small watersheds using the SWAT model, *Transactions of the ASAE*, 43,
24 1431-1439, 2000.

1 Stamati, F., Nikolaidis, N.P., Venieri, D., Psillakis, E. and Kalogerakis, N.: Dissolved organic
2 nitrogen as an indicator of livestock impacts on soil biochemical quality, *Applied*
3 *Geochemistry*, 26, S340-S343, 2011.

4 Stamati, F.E., Nikolaidis, N.P., Schnoor, J.P., Modeling topsoil carbon sequestration in two
5 contrasting agricultural soils – calibration issues and uncertainty analysis. *AGEE*, (In
6 Review), 2011.

7 Refsgaard, J.C.: Parameterisation, calibration and validation of distributed hydrological
8 models, *Journal of Hydrology*, 198, 69–97, 1997.

9 Rockstrom, J., Steffen, W., Noone, K., Persson, E., Chapin, F.S., Lambin, E.F., Lenton, T.M.,
10 Scheffer, M., Folke, C., Schellnhuber, H.J., Nykvist, B., de Wit, C.A., Hughes, T., van der
11 Leeuw, S., Rodhe, H., Sorlin, S., Snyder, P.K., Costanza, R., Svedin, U., Falkenmark, M.,
12 Karlberg, L., Corell, R.W., Fabry, V.J., Hansen, J., Walker, B., Liverman, D., Richardson, K.,
13 Crutzen, P. and Foley, J.A.: A safe operating space for humanity, *NATURE*, 461, 472-475
14 2009.

15 Roeckner, E., 2003. The atmospheric general circulation model ECHAM5. Part 1: Model
16 description , p. 127. Max Planck Institute for Meteorology Rep. 349, Hamburg, Germany,
17 127pp.

18 Rojas, R., Feyen, L., Dosio, A., Bavera, D.: Improving pan-european hydrological simulation
19 of extreme events through statistical bias correction of RCM-driven climate simulations,
20 *Hydrology and Earth System Sciences Discussions*, 8, 3883-3936, 2011.

21 Rozos, E., and Koutsoyiannis, D.: A multicell karstic aquifer model with alternative flow
22 equations, *Journal of Hydrology*, 325, 340-355, 2006.

23 Tritz, S., Guinot, V., and Jourde, H.: Modelling the behaviour of a karst system catchment
24 using non-linear hysteretic conceptual model, *Journal of Hydrology*, 397, 250-262, 2011.

1 Tzoraki, O. and Nikolaidis, N.P.: A generalized framework for modeling the hydrologic and
2 biogeochemical response of a Mediterranean temporary river basin. *Journal of Hydrology*,
3 346, 112-121, 2007.

4 Van Meijgaard, E., Van Ulft, L.H., Van De Berg, W.J., Bosveld, F.C., Van Den Hurk,
5 B.J.J.M., Lenderink, G. and Siebesma, A.P.: The KNMI regional atmospheric climate model
6 RACMO, version 2.1 KNMI-publication TR-302 KNMI, de Bilt, The Netherlands, 2008.

7 Wriedt, G., Van der Velde, M., Aloe, A., Bouraoui, F.: Estimating irrigation water
8 requirements in Europe. *Journal of Hydrology*, 373, 527-544, 2009.

9 Zhang, Z., Chen, X., Ghadouani, A., and Shi, P.: Modelling hydrological processes influenced
10 by soil, rock and vegetation in a small karst basin of southwest China, *Hydrological*
11 *Processes*, 25, 2456-2470, 2011.

12

1 Fig. 1. Geologic map of Koiliaris River basin boundary and estimated extended karst area.
2 Lines A1 and A2 depict the locations of the geologic cross sections presented in Fig. 2.
3
4 Fig. 2. Geologic cross sections of Koiliaris River Basin.
5
6 Fig. 3. Conceptual schematic of the karst model.
7
8 Fig. 4. Comparison of simulated flows with field data a) at the entrance of the gorge, b) the
9 exit of the gorge and c) the basin outlet used for model calibration.
10
11 Fig. 5. Comparison of simulated flows with field data a) at the basin outlet used for model
12 verification and b) long term simulation of the hydrology of the karst.
13
14 Fig. 6. Comparison of simulated nitrate concentrations with field data a) at the entrance of the
15 gorge and b) the basin outlet used for model calibration.
16
17 Fig. 7. Flush flood analysis of Keramianos Tributary at the gorge exit. a) Simulated daily
18 flow, b) maximum flow - flood exceedance frequency using all floods (1973-2010), and c)
19 maximum flow - flood exceedance frequencies for 1973-1996 and 1997-2010.
20

1 Fig. 8. Predictions of precipitation, ET (left) and flow (right) for Koiliaris River Basin under
2 the a) BCM_RCA, b) ECHAM_RACMO, and c) ECHAM_REMO climate change scenarios
3 for 1990-2050.

4

5 Fig. 9. Predictions of 20-year average (and standard deviation) precipitation, ET and flow
6 from the three climate change scenarios for Koiliaris River Basin.

7

Figure

[Click here to download high resolution image](#)

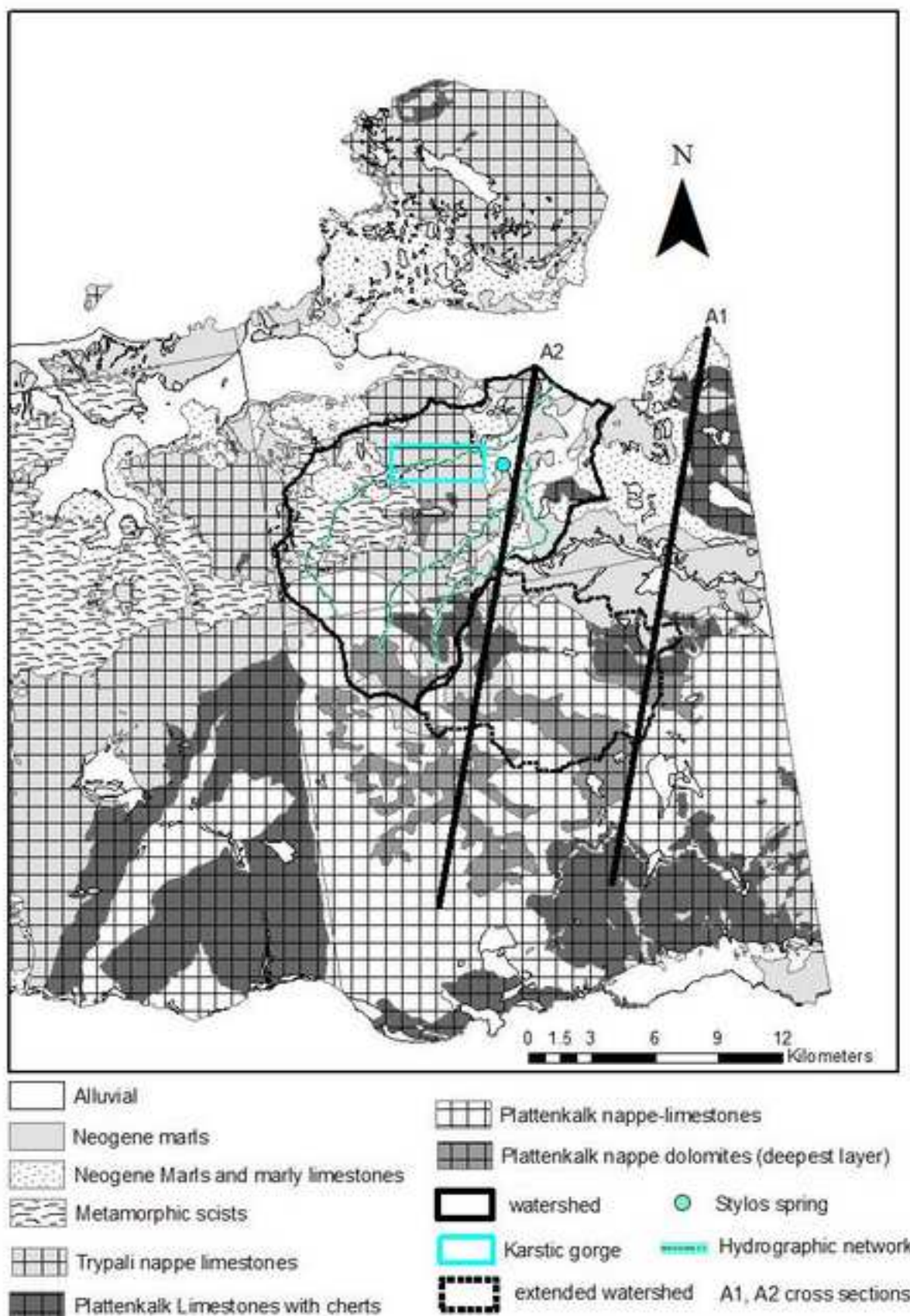
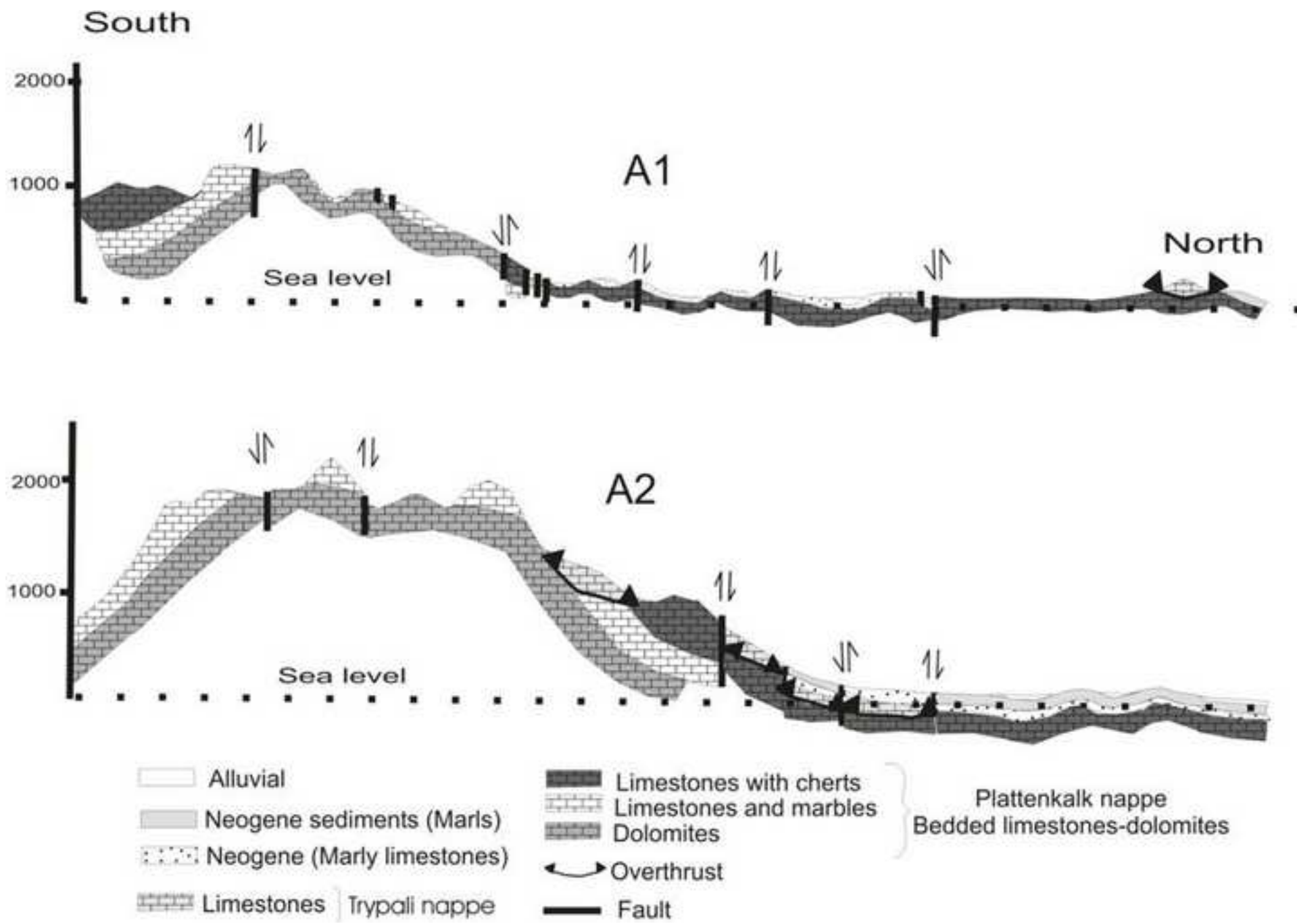
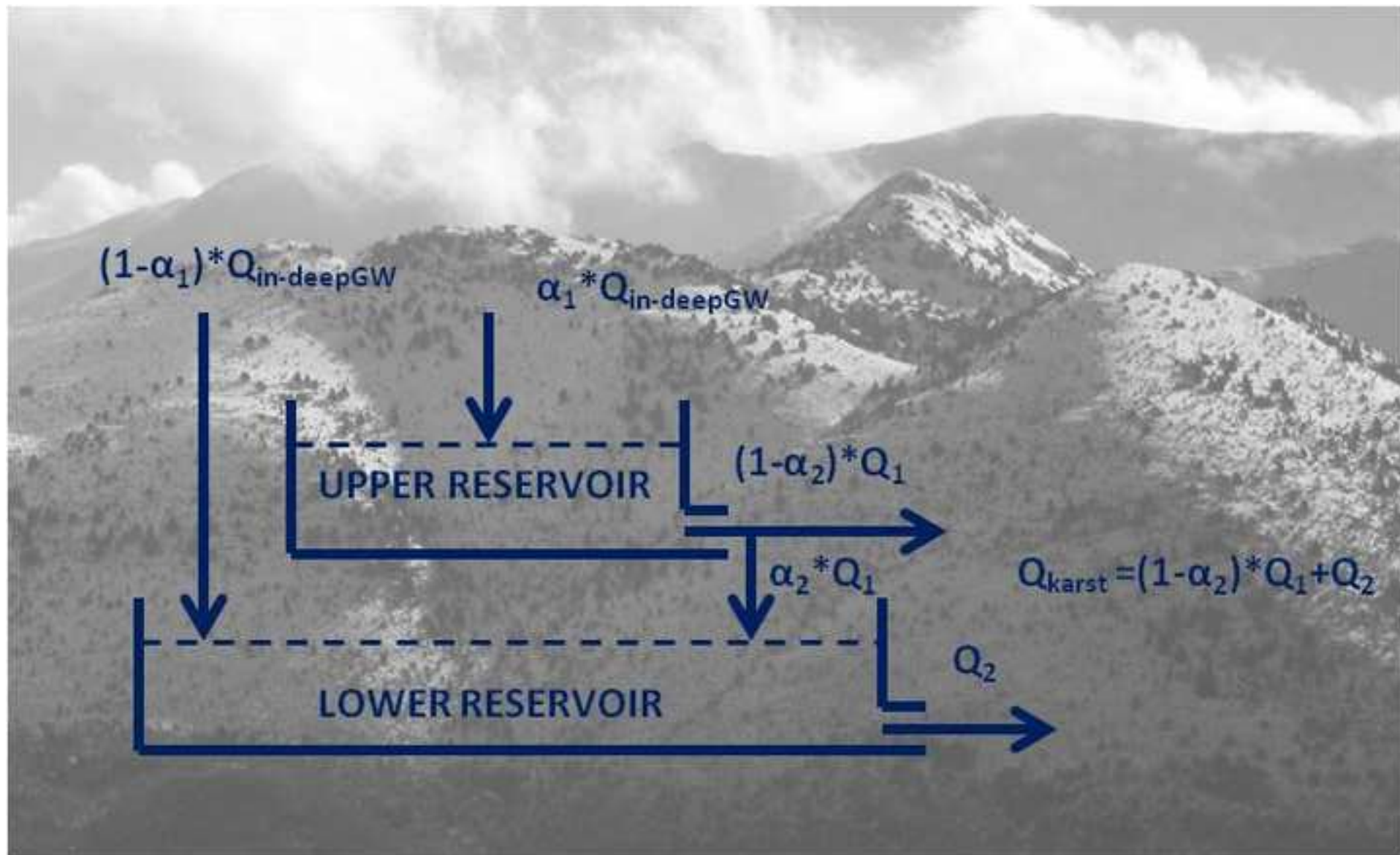


Figure
[Click here to download high resolution image](#)



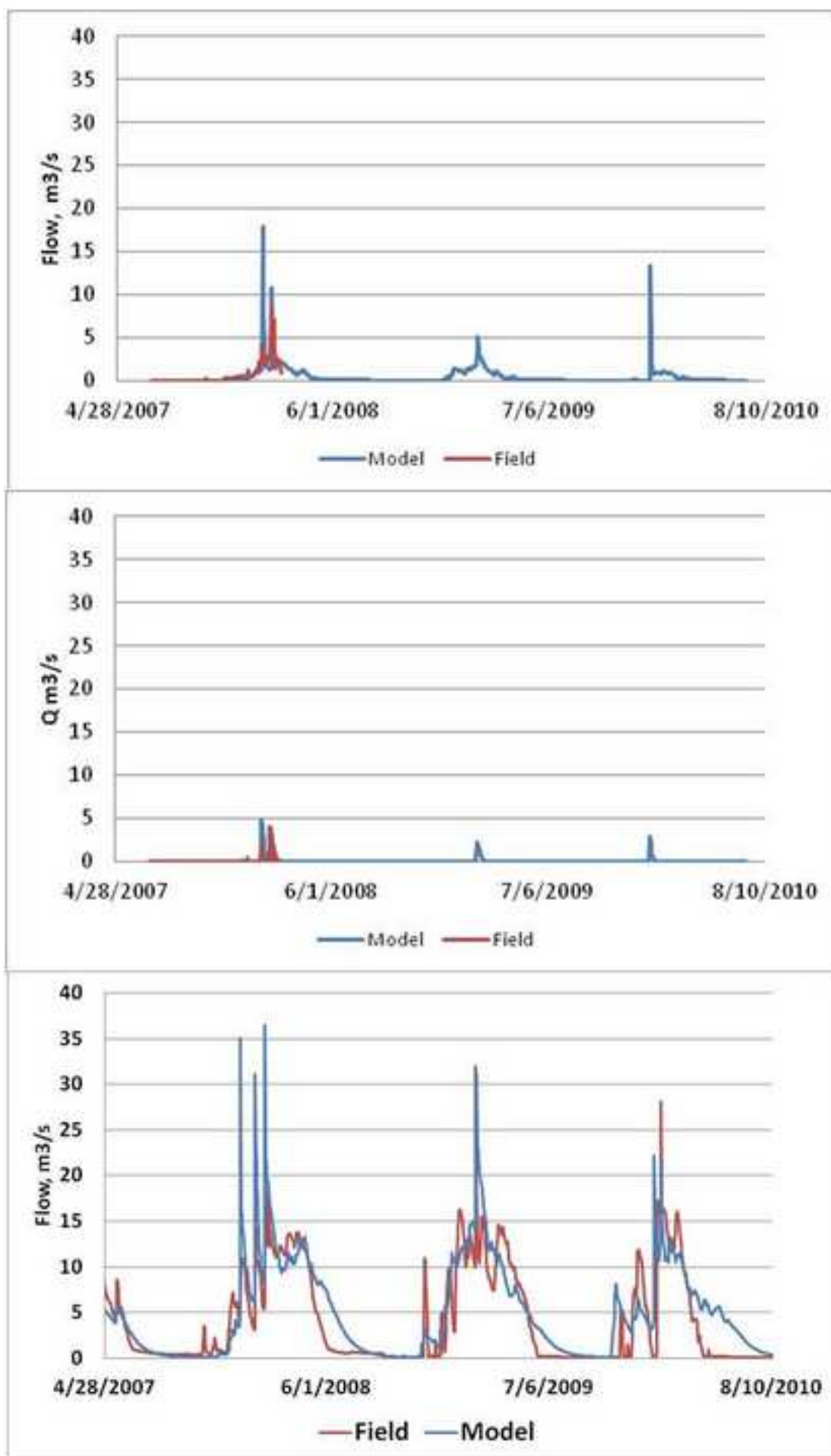
Figure

[Click here to download high resolution image](#)



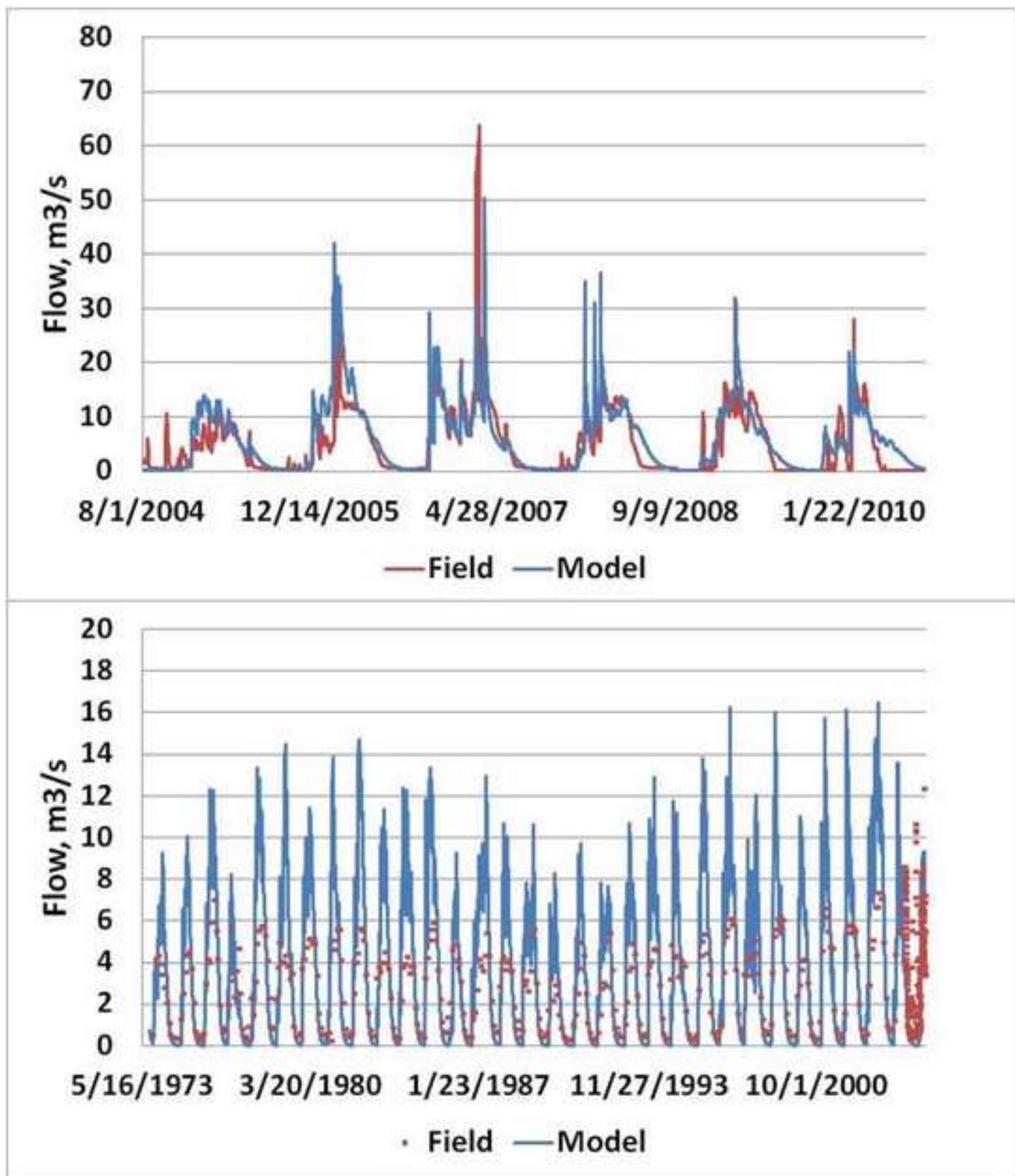
Figure

[Click here to download high resolution image](#)



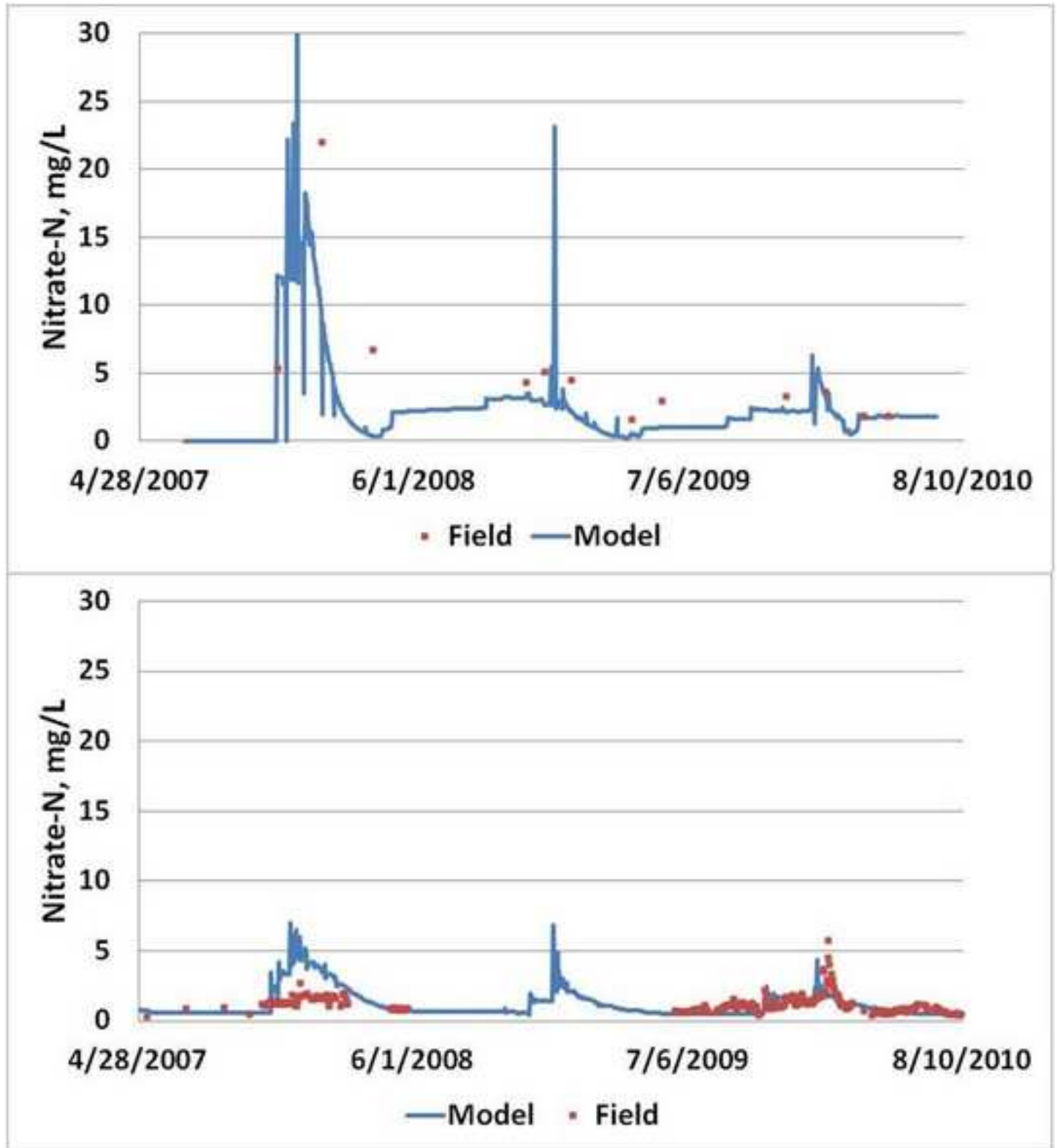
Figure

[Click here to download high resolution image](#)



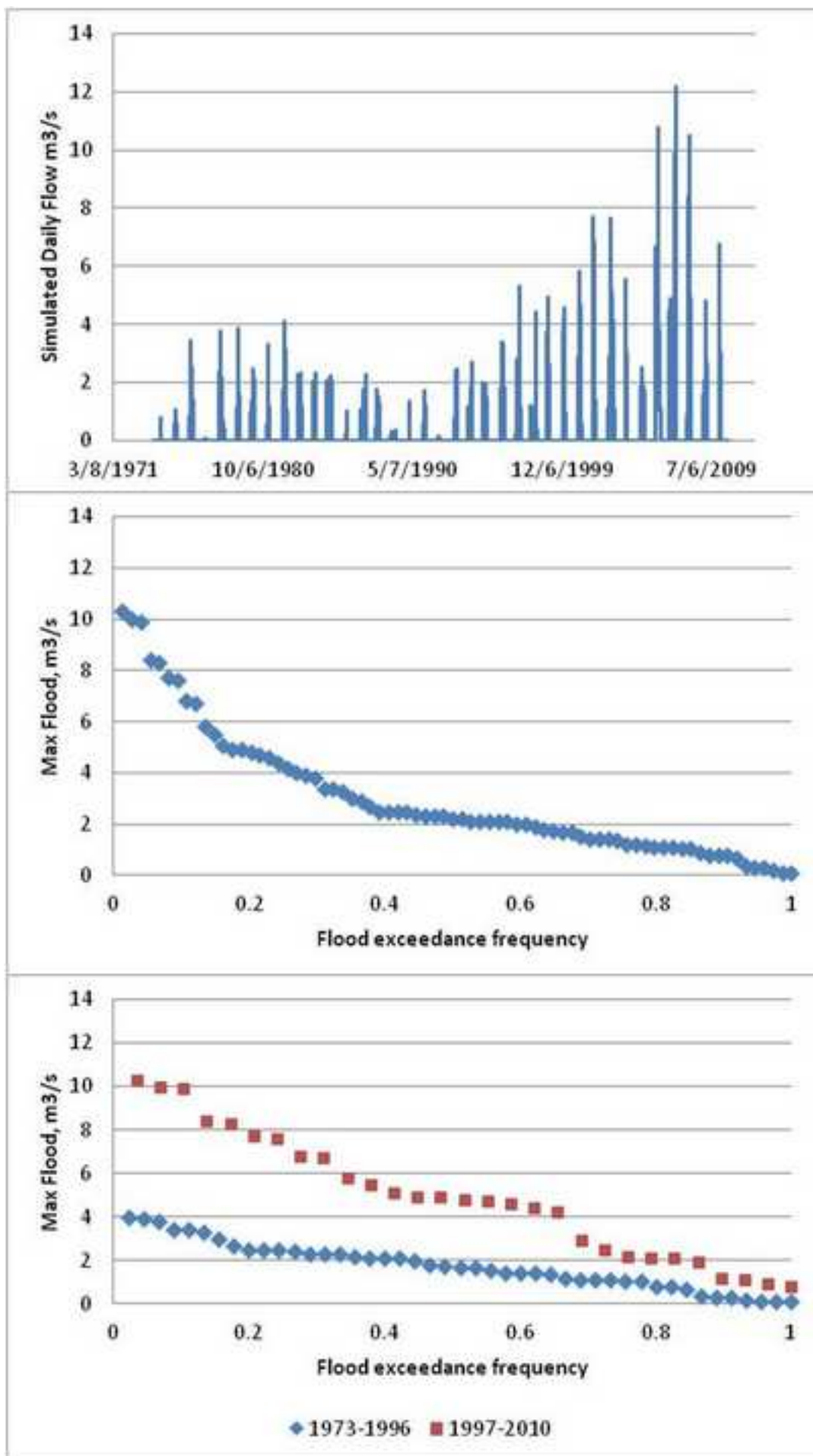
Figure

[Click here to download high resolution image](#)



Figure

[Click here to download high resolution image](#)



Figure

[Click here to download high resolution image](#)

